The Astrophysical Journal, 656:798 – 804, 2007 February 20

SPECTROPOLARIMETRY OF THE 3.4 μm ABSORPTION FEATURE IN NGC 1068

R. E. Mason
Gemini Observatory Northern Operations Centre, Hilo, HI; rmason@gemini.edu

G. S. Wright
UK Astronomy Technology Center, Royal Observatory Edinburgh, Blackford Hill, Edinburgh, UK; gsw@roe.ac.uk

A. Adamson
Joint Astronomy Centre, Hilo, HI; a.adamson@jach.hawaii.edu

and

Y. Pendleton
NASA Ames Research Center, Moffet Field, CA; ypendleton@mail.arc.nasa.gov
Received 2005 May 24; accepted 2006 October 16

ABSTRACT

In order to test the silicate-core/organic-mantle model of galactic interstellar dust, we have performed spectropolarimetry of the 3.4 μm C−H bond stretch that is characteristic of aliphatic hydrocarbons, using the nucleus of the Seyfert 2 galaxy, NGC 1068, as a bright, dusty background source. Polarization calculations show that if the grains in NGC 1068 had the properties assigned by the core-mantle model to dust in the Galactic diffuse interstellar medium (ISM), they would cause a detectable rise in polarization over the 3.4 μm feature. No such increase is observed. We discuss modifications to the basic core-mantle model, such as changes in grain size or the existence of additional nonhydrocarbon aligned grain populations, that could better fit the observational evidence. However, we emphasize that the absence of polarization over the 3.4 μm band in NGC 1068—and, indeed, in every line of sight examined to date—can be readily explained by a population of small, unaligned carbonaceous grains with no physical connection to the silicates.

Subject headings: astrochemistry — dust, extinction — galaxies: individual (NGC 1068) — galaxies: ISM — galaxies: Seyfert — polarization

1. INTRODUCTION

In our Galaxy, and no doubt others, stars and planets form from components available in the local interstellar medium (ISM). The organic compounds observed in interstellar space may therefore be the first step toward the complex materials that help make planets habitable. A greater understanding of the origin and evolution of the organic materials in the ISM, both in our Galaxy and in others, is thus of great interest.

Particularly puzzling are the aliphatic hydrocarbons, whose presence in the diffuse ISM (DISM) of the Milky Way has been established through observations of C−H bond stretches near 3.4 μm, seen in absorption throughout the DISM of our own Galaxy and others (Sandford et al. 1991, 1995; Pendleton et al. 1994; Imanishi 2000; Rawlings et al. 2003; Risaliti et al. 2003; Dartois et al. 2004; Mason et al. 2004). Two very different models exist to explain the production of this material: photoprocessing of the icy dust grain mantles found in dense molecular clouds (e.g., Li & Greenberg 1997), and hydrogenation in the DISM of small, amorphous carbon particles of the kind produced in outflows from evolved stars (e.g., Mennella et al. 2002). As the former process would result in the 3.4 μm band of DISM hydrocarbons arising in organic mantles on silicate grain cores, it is commonly known as the "core-mantle" dust model.

Both of these models are to some extent consistent with the observational data. For instance, laboratory experiments mimicking both dust formation pathways have succeeded in producing materials with 3.4 μm bands that are a good match to the astronomical feature (Greenberg et al. 1995; Mennella et al. 1999, 2002), although the critically diagnostic 5–10 μm region reveals a much closer match between observations and hydrogenated amorphous carbon materials (Chiar et al. 2000; Pendleton & Allamandola 2002). The presence of the 3.4 μm band in proto–planetary nebulae (Chiar et al. 1998) shows that hydrocarbon solids can be produced in circumstellar regions, while the attribution of the 6 μm excess absorption in protostars to organic refractory material (Gibb & Whittet 2002) would, if confirmed, indicate that ice processing can also produce some fraction of the hydrocarbons. The organic OCN^- band at 4.62 μm provides evidence of ice processing in such environments (Demyk et al. 1998; Pendleton et al. 1999).

Spectropolarimetry provides opportunities for clearly discriminating between these scenarios. In the core-mantle model, the silicate core/organic mantle grains are responsible for the bulk of the visual and IR extinction and all of the polarization in the DISM (Li & Greenberg 1997). As the polarization is caused by dichroic absorption, we would therefore expect to observe polarization of the continuum with an increase in polarization over absorption features associated with the grains (e.g., Hough et al. 1988; Pendleton et al. 1990; Smith et al. 2000). Specifically, increases in polarization must occur simultaneously over the 3.4 μm "mantle" feature and the 9.7 μm absorption characteristic of the silicate core, with roughly comparable efficiency (Li & Greenberg 2002). This was first investigated by Adamson et al. (1999), who compared the polarization over the 3.4 μm feature toward the Galactic center source IRS 7 with that of the 9.7 μm band toward the nearby Galactic center source IRS 3. The increase in polarization over the 3.4 μm absorption was found to be $\lesssim$0.08%, much less than the 0.4% expected on the basis of the silicate feature polarization, in apparent conflict with the core-mantle model.

However, as pointed out by Li & Greenberg (2002) the silicate-feature polarization used in that work, while arising toward an object at a projected distance of about 0.25 pc from that toward

which the 3.4 μm polarization was measured (Geballe et al. 1989), does not refer to exactly the same line of sight, admitting the possibility that the silicate feature in the diffuse ISM toward IRS 7 may be less polarized than expected. Studies of additional lines of sight (at a lower signal-to-noise ratio and/or spectral resolution), while reaching similar conclusions to those of Adamson et al. (1999), suffer from similar limitations (Nagata et al. 1994; Ishii et al. 2002). More recently, Chiar et al. (2006) measured the polarization of both the hydrocarbon and silicate features toward the Quintuplet cluster in the Galactic center, finding the hydrocarbons to be significantly less polarized than would be expected if they existed as mantles on the polarized silicate grains.

To provide another data point against which the predictions of the core-mantle grain model can be compared, and to extend this study to a new and different environment, we have used the bright nucleus of the Seyfert 2 galaxy NGC 1068 as a source against which to measure the polarization of the 3.4 μm band and the continuum around it. Rather than the 10 μm silicate feature, we have used the degree of continuum polarization to calculate the enhancement in polarization that would be expected over the 3.4 μm feature from a screen of elongated, coated silicate grains that polarize by the selective absorption of one plane of the incident light. In § 2, we describe the line of sight toward the nucleus of NGC 1068 and its suitability for this work. The spectropolarimetric observations and their treatment are outlined in § 3. The calculations that we have carried out are discussed in § 4, and the results presented in § 5. This work is then summarized in § 6.

2. DUST AND DICHROIC POLARIZATION IN NGC 1068

As the archetypal Seyfert 2 galaxy, NGC 1068 ($d = 16$ Mpc; $H_0 = 70$ km s^{-1} Mpc^{-1}; $1'' = 72$ pc) has been the center of much attention. The unified model of active galactic nuclei (AGNs) implies that the galaxy harbors a Seyfert 1 nucleus, obscured from our point of view by a torus of dust and molecular gas, and 10 μm interferometry (Jaffe et al. 2004), as well as the detection of broad emission lines in polarized light (Antonucci & Miller 1985), have provided strong evidence for the existence of such a torus. Copious other mid-IR and X-ray data also show that the nucleus of NGC 1068 is obscured by large amounts of warm dust (e.g., Bock et al. 2000; Matt et al. 2000; Tomono et al. 2001; Alloin et al. 2000; Mason et al. 2006). While the classification of NGC 1068 as a type 2 object suggests that the obscuring torus is oriented roughly edge-on to our line of sight, the disk of the galaxy has quite a low inclination ($i \approx 29^\circ$; García-Gómez et al. 2002). This means that the line of sight to the center of NGC 1068 samples dust local to the active nucleus, with a negligible contribution from dust in the disk of the galaxy.

The 3.4 μm absorption band has been observed in NGC 1068 (Bridger et al. 1994; Wright et al. 1996; Imanishi et al. 1997; Marco & Brooks 2003; Mason et al. 2004), as has silicate absorption at 9.7 μm (Kleinmann et al. 1976; Roche et al. 1984; Jaffe et al. 2004; Mason et al. 2006; Rhee & Larkin 2006). The 3.4 μm band has a profile very similar to that observed in Galactic lines of sight; although the band carrier exists in the central region of an active galaxy, it apparently undergoes little extra processing compared to the Galactic DISM (Dartois et al. 2004; Mason et al. 2004). NGC 1068 has a nuclear dust spiral that appears physically connected to the galaxy disk (Pogge & Martini 2002), so it is quite possible that the hydrocarbons in the nucleus of NGC 1068 formed in the disk of the galaxy and then migrated to the center. We therefore proceed on the assumption that the hydrocarbon-containing dust in the nucleus of NGC 1068 initially formed by one of the mechanisms that has been suggested to be responsible for Galactic aliphatic hydrocarbons.

The nucleus of NGC 1068 is known to be polarized from the UV to the mid-IR, and the mechanisms responsible for this polarization have been the subject of intense study. Antonucci & Miller (1985) were among the first to observe the UV and visible polarization of NGC 1068, and they interpreted the high, wavelength-independent polarization as being due to scattering off very small particles, probably free electrons. Bailey et al. (1988) later discussed the polarization properties of NGC 1068 from the UV out to 10 μm and found a twist in position angle from the optical into the near-IR. They interpreted this as dust or electron scattering being replaced by dichroic absorption, the preferential absorption of one component of the electric vector, as the most important polarizing mechanism. Their data also show a change of $\sim 70^\circ$ in position angle between the *L* and *M* bands, consistent with dichroic emission from aligned dust grains becoming the dominant polarizing mechanism at longer wavelengths.

Further evidence for the importance of dichroic absorption as a polarizing mechanism in the IR comes from imaging polarimetry. After analyzing the deviations from the centrosymmetric patterns expected from scattering alone, Lumsden et al. (1999) concluded that their data required another mechanism of constant position angle contributing to the polarization. The effect of this mechanism grows with increasing wavelength, as would be expected if absorption were beginning to dominate over scattering, and was estimated to account for >90% of the *K*-band polarization. Lumsden at el. were successful in fitting their observed *JHK*-polarized flux points with graybody emission from hot ($T \sim 1200$ K) dust, reddened by a $\lambda^{-1.75}$ extinction curve and scaled by a Serkowski law appropriate for moderately extinguished Galactic sources. Furthermore, Packham et al. (1997) interpreted the different aperture dependences of the *J*-, *H*-, and *K*-band polarizations as consistent with a dichroic contribution in the *H* and *K* bands. With higher resolution *Hubble Space Telescope* imaging polarimetry, Simpson et al. (2002) also found that the *K*-band polarization has a contribution from dichroism, but they were able to set tighter limits on the location of the dichroic component, to within $1''$ of the nucleus.

This agrees with the more detailed modeling of Young et al. (1995), who find that neither electron nor dust scattering can account for the near-IR polarization of NGC 1068. However, if a dichroic component is added, the near-IR polarized flux spectrum can be reproduced. In this model, there is still some contribution from electron scattering to the near-IR flux, but this decreases with wavelength relative to the dichroic component. By the *K* band, electron scattering contributes perhaps 10% of the total flux, with dust making up almost all of the remainder. At *L*, the scattering contribution in their model would be negligible.

Watanabe et al. (2003) are also successful in modeling the near-IR polarization of NGC 1068 with polarization from aligned dust grains. In addition, they raise the possibility that the IR polarization could be caused by scattering off large grains in the torus, and point out that neither the 70° change in position angle nor the absence of a centrosymmetric scattering pattern at longer wavelengths necessarily rules out scattering as the polarizing mechanism. This has yet to be tested in any detail, but the implications that it may have for the conclusions of this study are discussed in § 5.

While the near-IR data point to dust absorption being the dominant polarizing mechanism in the *L* band, spectropolarimetry of the 9.7 μm silicate feature does not show the pronounced polarization excess that might be expected if emission or absorption from aligned silicates were causing the polarization (Aitken et al. 1984). This observation was interpreted as evidence that the mid-IR polarization arises in emission from nonsilicate grains or

has a nonthermal origin. However, the lack of polarization in the silicate feature does not necessarily rule out the presence of aligned silicate-core grains in the nucleus of NGC 1068. In radiative transfer calculations of dichroic polarization from silicate-containing grain mixtures in dusty disks, Efstathiou et al. (1997) and Aitken et al. (2002) find numerous configurations in which the polarization over the feature is in fact quite flat, consistent with the observations of Aitken et al. (1984).

Although it appears possible for radiative transfer effects to suppress the silicate feature polarization, the shorter wavelength 3.4 μm band should be much less affected by such interplay between absorption and emission. The ratio of the optical depths of the 3.4 and 9.7 μm bands in NGC 1068 supports this suggestion. In the five Galactic lines of sight examined by Sandford et al. (1995), there is a fair degree of correlation between the depths of the two features ($\tau_{9.7}/\tau_{3.4} = 13-19$, with the higher values toward the Galactic center), but in NGC 1068 $\tau_{9.7}/\tau_{3.4} \approx 5$, suggesting that the 3.4 μm band is indeed less affected by underlying emission than is the silicate feature. This further suggests that treating the dust producing the 3.4 μm band as a uniform absorbing screen (an assumption implicit in the calculations outlined in § 4), while undoubtedly a major simplification of the dust geometry and temperature structure in this AGN, is still a useful approximation. Overall, imaging polarimetry, spectral modeling, and the near-90° rotation in position angle all imply that a model of the *L*-band polarization of NGC 1068 based on selective dust absorption is a reasonable representation of the true situation.

3. OBSERVATIONS AND DATA REDUCTION

L-band spectropolarimetry of the nucleus of NGC 1068 was obtained on the nights of 2000 September 19 and 2000 October 6 using the IRPOL2 spectropolarimetry module and CGS4 on the 3.8 m UK Infrared Telescope on Mauna Kea, Hawaii. The 40 l mm^{-1} grating and 0.6″-wide slit were used, providing $R = 1360$ at 3.4 μm. The weather conditions were good during the second night, but some thin cirrus was present on the first.[1]

In order to obtain Stokes *Q* and *U* parameter spectra, a frame was taken with IRPOL2's half-wave plate at each of four positions: 0°, 45°, 22.5°, and 67.5°. This cycle was repeated 64 times in all. At each of these wave-plate angles, ordinary and extraordinary beams were extracted from the sky-subtracted frames, stacked together, and the final, total spectra combined using the "ratio" method (see, e.g., Tinbergen 1996) to produce Stokes *Q* and *U* parameter spectra. This method has the advantage of minimizing the effects of variations in sky transmission during the observations.

Prior to calculation of the polarization, further treatment of the raw *Q* and *U* spectra was necessary. First, data points between 3.3 and 3.4 μm (observed) were rejected. This part of the spectrum contains deep absorptions from the hydrocarbon cement in IRPOL2's Wollaston prism (at 3.35–3.4 μm) and from atmospheric methane (3.31–3.33 μm), and these lines do not ratio out at all satisfactorily.

A second effect that must be dealt with is a large-amplitude ripple in the spectrum, which is thought to be caused by multiple reflections in the waveplate. The ripple was removed using the fast Fourier transform (FFT) technique described by Adamson et al. (1999). Briefly, the ripple causes peaks to appear around 0.5 and 1.0 times the Nyquist frequency in the Fourier transform of the spectrum. These peaks were set to zero, then the transform was inverted. The instrumental zero point of polarization was determined and removed from the NGC 1068 *Q* and *U* spectra using observations of the unpolarized star HD 18803 (Clayton & Martin 1981), and the resulting polarization spectrum corrected for the imperfect efficiency of the waveplate.[2] The position angle of polarization (PA) was calibrated using observations of the young stellar object AFGL 2519, whose PA at 3–4 μm was previously measured by Hough et al. (1989). An intensity spectrum was also constructed using only a few frames taken near in time to HD 18803, which was used as a telluric standard. The polarization, position angle, and total flux spectra of NGC 1068 are shown in Figure 1, together with the polarimetric results of Bailey et al. (1988) and Lebofsky et al. (1978).

4. POLARIZATION CALCULATIONS

To calculate the *L*-band polarization produced by coated dust grains, we have taken advantage of the discrete dipole approximation (DDA) code, DDSCAT6.1 (Draine 1988; Draine & Flatau 1994, 2004). In the DDA, the dust grain is represented as an array of dipole oscillators on a cubic lattice, and absorption, scattering, and extinction cross sections are then calculated from the amplitudes of the dipoles as they interact with the incident electric field.

The optical constants adopted for the grain cores and mantles are those of the "astronomical silicate" (Draine & Lee 1984; Draine 1985; Weingartner & Draine 2001) and the organic refractory material of Li & Greenberg (1997). The refractive index of the organic component is derived from the Murchison meteorite and laboratory residues exposed to the solar UV field aboard the *EURECA* satellite (Greenberg et al. 1995; Greenberg & Li 1996). While both of those materials show absorption bands at 5–9 μm that are not seen in the diffuse ISM (Pendleton & Allamandola 2002), the 3.4 μm bands of both bear a good resemblance to the observed feature.

The existence of polarization caused by dust absorption indicates that the dust grains must be aspherical, but beyond that their shapes are not well established. We have treated the dust grains as oblate spheroids with an axial ratio of 2:1, the cores and mantles having equal eccentricities. Based on fits to the Trapezium 9.7 μm silicate feature, Draine & Lee (1984) find that 2:1 oblate spheroids are a reasonable representation of dust grains, and Hildebrand & Dragovan (1995) also favor oblate over prolate spheroids. They conclude that the axial ratio must be $<3:1$, with a best-fitting value of 1.5:1. There has been some dispute over whether oblate or prolate spheroids give a better fit to the observational data (Greenberg & Li 1996), but we note that the main discrepancy in the polarization predicted by these two shapes comes over the 9.7 μm silicate feature. The differences are small at the wavelengths of interest in this work (see Fig. 6 of Draine & Lee 1984). The elongation of the grains will affect the efficiency with which they polarize, but will have little effect on the wavelength dependence of the polarization (Greenberg & Li 1996).

We have adopted simple picket-fence alignment for this work (which is equivalent to the perfect spinning alignment approximation for oblate grains), with the grains' short axes orientated perpendicular to the direction of propagation of the incident light. This has been shown to be quite adequate if only the wavelength dependence of the polarization is required, rather than its absolute value (Chlewicki & Greenberg 1990). The functional form used for the grain size distribution is the MRN $a^{-3.5}$ power law with limits of 0.005 and 0.25 μm (Mathis et al. 1977).

[1] Spectropolarimetry of the 9.7 μm silicate feature was later also attempted, but poor weather meant that none of the data obtained were useful.

[2] As given by http://www.jach.hawaii.edu/UKIRT/instruments/irpol/CGS4/cgs4pol.html#5.

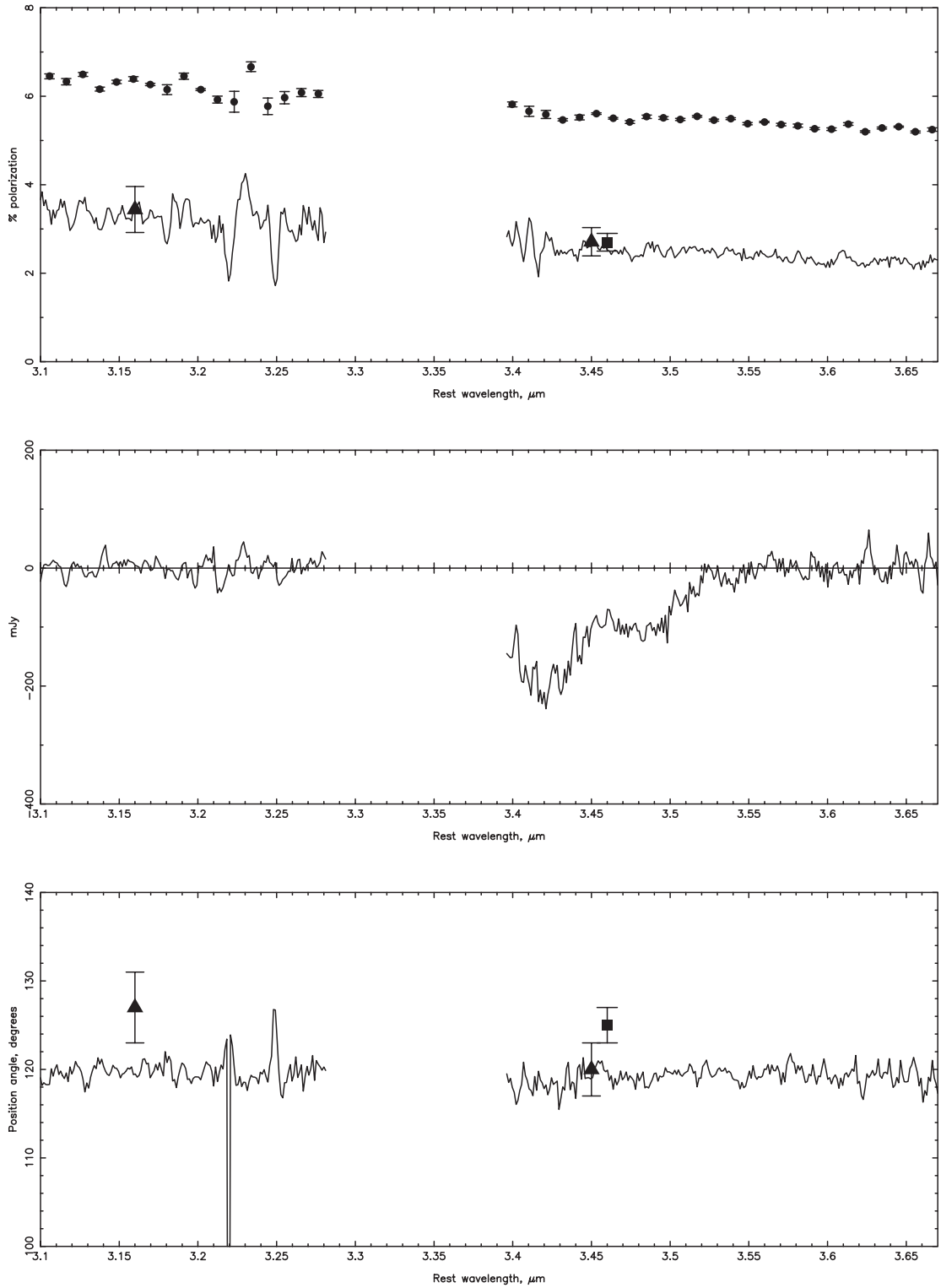

FIG. 1.— *Top*: *L*-band polarization spectrum of NGC 1068. The binned spectrum was obtained by calculating the standard error of the *Q* and *U* spectra in 0.010 μm bins and is offset by 3% for clarity. Also shown are the measurements of Bailey et al. (1988; *triangles*) and Lebofsky et al. (1978; *square*, offset by 0.01 μm in wavelength). *Middle*: Continuum-subtracted flux spectrum, showing the peak of the 3.4 μm absorption feature. *Bottom*: Position angle of polarization, with the measurements of Bailey et al. (1988) and Lebofsky et al. (1978), as above.

Given this information about the size, shape, composition, and orientation of the grains, DDSCAT calculates a number of quantities. Those relevant to this work are

$$Q_{\rm abs} = C_{\rm abs}/\pi a^2, \quad (1)$$

$$Q_{\rm sca} = C_{\rm sca}/\pi a^2, \quad (2)$$

$$Q_{\rm ext} = Q_{\rm abs} + Q_{\rm sca}, \quad (3)$$

$$Q_{\rm pol} = Q_{\rm ext,\parallel} - Q_{\rm ext,\perp}, \quad (4)$$

in which Q are efficiencies and C are cross sections for absorption, scattering, and extinction and $Q_{\rm ext,\parallel}$ and $Q_{\rm ext,\perp}$ refer to extinction efficiencies for the two orthogonal incident polarization states (Draine 1988).

From $Q_{\rm ext}$ and $Q_{\rm pol}$, extinction and polarization spectra for ensembles of grains can be obtained in the following manner:

$$\tau(\lambda) = N_{\rm grain} \int_{a_{\rm min}}^{a_{\rm max}} n(a) C_{\rm geo} Q_{\rm ext}(a, \lambda)\, da, \quad (5)$$

$$p(\lambda) = N_{\rm grain} \int_{a_{\rm min}}^{a_{\rm max}} n(a) C_{\rm geo} \frac{Q_{\rm pol}}{2}(a, \lambda)\, da, \quad (6)$$

where $C_{\rm geo}$ is the geometrical cross section of the grain in question, $N_{\rm grain}$ is the column density of grains [with $n(a)$, the number of grains in the interval $a, a + da$, appropriately normalized], and $a_{\rm min}$ and $a_{\rm max}$ are the limits of the size distribution to be considered.

5. RESULTS AND DISCUSSION

We are interested in the magnitude of any increase in polarization that would be expected over the 3.4 μm absorption band, given a certain continuum polarization caused by dichroic absorption by core-mantle grains. To obtain a crude estimate of the polarization that might be expected over the 3.4 μm band, we can consider the polarization observed over the 9.7 μm silicate band in Galactic lines of sight. For a given grain shape, size, and composition, changes in abundance and degree of alignment will alter the level of continuum polarization without affecting the ratio of feature to continuum polarization, $P_{\rm feat}/P_{\rm cont}$. In Galactic lines of sight that can be fitted with pure absorptive polarization, this ratio is typically about 3–4, with a couple of objects reaching values of $\sim$7 (OMC-1 BN, Sgr A GCS3 II; Smith et al. 2000). Alternatively, the optical constants of astronomical silicate give rise to $P_{\rm feat}/P_{\rm cont} \approx 12$ (Draine & Lee 1984; Hildebrand & Dragovan 1995). The "excess" polarization over an absorption feature is determined by the strength of the band, and Li & Greenberg (2002) have shown that silicates and hydrocarbons polarize to a similar degree per unit optical depth. Observed values of $\tau_{9.7}/\tau_{3.4}$ range from $\sim$13–19 (Sandford et al. 1995), implying $P_{\rm feat}/P_{\rm cont} \sim$ 1.15–2.0 in the 3.4 μm band. For NGC 1068, where the L-band continuum polarization is about 2.5%, this translates to peak polarizations of 2.9%–5% across the 3.4 μm feature. This suggests that a significant excess polarization should be detectable over the 3.4 μm feature, although the spread in silicate feature polarizations and $\tau_{9.7}/\tau_{3.4}$ and the fact that most of the sources in Smith et al. (2000) are dominated by molecular cloud material mean that these numbers should be treated with some caution.

To estimate the likely maximum observed polarization change over the 3.4 μm band in NGC 1068, the best-fitting linear continuum was first found for the polarization data. A model polarization spectrum was then created from the optical depth spectrum derived from the spectropolarimetry data, assuming that $p \propto \tau$. The model spectrum was normalized to the continuum around 3.55 μm, then scaled by various factors, and the reduced χ^2 between it and the binned polarization spectrum calculated for each scaling. The best fit corresponds to a deviation of $-0.12 \pm 0.25\%$ (95% confidence) from the linear continuum; the data are in fact consistent with a small *decrease* in polarization over the 3.4 μm feature. The model fit giving the upper limit on the change in polarization over the 3.4 μm band (i.e., peaking at 0.13% above the continuum) is shown in Figure 2.

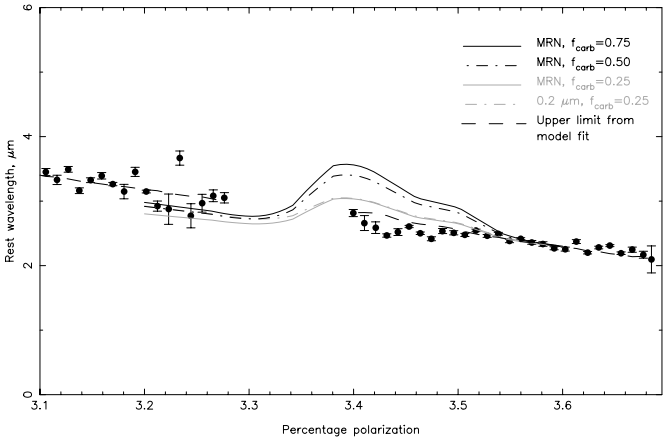

FIG. 2.—Observed and predicted polarization over the 3.4 μm feature in NGC 1068 for an MRN distribution of coated silicate particles with different thicknesses of mantle. Also shown are the polarization of a 0.2 μm grain ($f_{\rm carb} = 0.25$), close to the largest size in the MRN distribution, and the limit on the change in polarization over the feature, based on a model fit to the observed polarization (see text). The column density of grains (eq. [6]) was chosen to reproduce the observed polarization around 3.55 μm, a region expected to be unaffected by the 3.4 μm feature.

The polarization calculated as described in § 4 for a population of core-mantle grains with the MRN size distribution is also shown in Figure 2. As grain size may affect the magnitude of the 3.4 μm polarization excess (§ 5.1), the polarization from a 0.2 μm grain, close to the largest size in the MRN distribution and somewhat larger than the average $\langle a \rangle = 0.087$ μm of the finite cylinders in the Li & Greenberg (1997) model, is also shown. The different curves in the figure result from different values of $f_{\rm carb}$, the fraction of the grain volume that is contained in the mantle. Various figures have been suggested for this quantity: Li & Greenberg (2002) consider $f_{\rm carb} = 0.2$, 0.5, and 0.75, while according to Chlewicki & Greenberg (1990) $f_{\rm carb} \sim 0.9$. Greenberg & Li (1996) and Li & Greenberg (1997) estimate mantle/core volume ratios of about 2:1. As expected, the polarization at the peak of the 3.4 μm band increases with the amount of carbonaceous material in the grains, from $\sim$3.0% for the 25%-mantle MRN grains, to $\sim$3.6% for the 75%-mantle particles.

For the core/mantle ratios closest to those most commonly quoted in the literature, the 3.4 μm polarization predicted by the model is clearly well in excess of the observed polarization. In the case of the grains with only 25% of the volume contained in the mantle, the polarization at the peak of the 3.4 μm absorption is 0.29% over the linear continuum fit mentioned above. This is still somewhat above the limit we derive on the observed polarization; the expected and observed polarizations are not reconciled even with only a small fraction of each grain being composed of organic refractory material. The core-mantle grain model, at least in the form proposed for the Galactic diffuse ISM, is unlikely to explain the L-band polarization of NGC 1068.

5.1. *Variations on the Basic Core-Mantle Model*

Are there likely to be significant differences in the grain population(s) in NGC 1068 that might diminish the amount of polarization expected over the 3.4 μm band, even while core-mantle grains are present? The similarity of the band profile in NGC 1068 and the Galactic diffuse ISM suggests that the composition of the hydrocarbon material is similar in both galaxies (Dartois et al. 2004; Mason et al. 2004), but other differences may arise. For instance, as the Li & Greenberg (1997) model proposes that the entire infrared polarization arises in the core-mantle grains, we have so far also assumed this, but if another, non–hydrocarbon-containing aligned grain component also contributed to the polarization in NGC 1068 it would diminish the size of the rise in polarization expected over the 3.4 μm band, while contributing to A_V but not $\tau_{3.4}$. In NGC 1068, such a second polarizing grain population could conceivably be, for example, bare silicates arising from destruction of the mantles on some fraction of the grains.

Values of extinction for the complex, infrared-emitting regions of the nucleus of NGC 1068 may not be as straightforward to interpret as the extinction through the large column of cold dust toward the Galactic center, but estimates range from $\sim$15 (Lumsden et al. 1999; Watanabe et al. 2003) to $\sim$40 (Young et al. 1995), disregarding values based on $\tau_{3.4}$. Given that $\tau_{3.4} \approx 0.1$, this implies that $A_V/\tau_{3.4} \sim 150-400$, compared with Galactic values of $\sim$150 (toward the Galactic center; Pendleton et al. 1994) or several hundred (toward field stars at various Galactic longitudes; Rawlings et al. 2003). There is therefore no compelling reason to think that grain components other than those proposed for the Galactic diffuse ISM must exist in NGC 1068, but the wide range of estimates of $A_V/\tau_{3.4}$ for both the Galactic and extragalactic lines of sight means that this cannot be ruled out either.

Another issue that could affect the 3.4 μm band in both extinction and polarization is that of grain size. Increasing grain size tends to increase the efficiency of continuum extinction while decreasing the strength of absorption features, so large grains might be able to polarize the L-band continuum effectively without producing much excess polarization through the 3.4 μm band. For grains much larger than $\sim$0.2 μm in radius, scattering starts to become important ($Q_{\rm abs}/Q_{\rm sca} \approx 5$ for a 0.2 μm core-mantle 2:1 oblate spheroid at 3.3 μm) and calculations of the polarization from such particles in a complex system like NGC 1068, where the inclination of the dusty torus and multiple scattering effects may be critical, are beyond the scope of this paper.

It has been suggested that dust grains in AGNs may be biased toward larger sizes than in the diffuse ISM, but the evidence remains contradictory. Laor & Draine (1993) pointed out that large ($\sim$10 μm) dust grains are likely to survive longer than small grains close to an AGN and will not produce a silicate emission feature. The weakness or absence of silicate emission in type 1 AGNs prompted the inclusion of large grains in some torus models (van Bemmel & Dullemond 2003), but its recent discovery in several quasars may argue against large grains (Hao et al. 2005; Siebenmorgen et al. 2005). Flat $L - M'$ colors, peculiar $E_{B-V}/N_{\rm H}$ and $A_V/N_{\rm H}$ ratios in Seyfert 2 nuclei, and the absence of the 2175 Å feature in reddened Seyfert 1 galaxies have all been interpreted as evidence for large grains (Imanishi 2001; Maiolino et al. 2001a, 2001b), but geometrical effects may also be able to explain many of these observations (Weingartner & Murray 2002). In the specific case of NGC 1068, both Young et al. (1995) and Watanabe et al. (2003) were able to fit the observed J- to K-band and optical polarization with grain sizes no different from those thought to exist in the Galactic DISM, although Watanabe et al. suggest that scattering from large grains in the torus might be a viable alternative. If extended to the 3.4 μm band, detailed extinction and polarization calculations such as those of Watanabe et al. (2003) could provide valuable constraints on both the size and structure of the grains in AGN tori.

Finally, we note that if the grain size distribution is biased toward larger sizes in NGC 1068, this could be through preferential destruction of small grains, or large grains may have grown by coagulation in this warm, dense environment. If the latter, then they may have lost some of their former core-mantle nature. It seems likely that small hydrocarbon inclusions in large, coagulated grains would leave their polarization signature on the 3.4 μm band, but again, further calculations would be needed to test this.

5.2. *Hydrocarbon Formation in the Diffuse ISM*

The absence of excess polarization over the 3.4 μm band can be naturally explained if the feature arises in a population of grains that does not contribute significantly to the continuum polarization. Such a grain population must be small and/or optically isotropic (small grains being harder to align than large ones; Lazarian 2003 and references therein) and have no physical connection to the silicate grains. Recent laboratory work has provided persuasive evidence that small carbon grains like those thought to be ejected from asymptotic giant branch stars can be hydrogenated during the later stages of stellar evolution (Schnaiter et al. 1999), in the diffuse ISM (Mennella et al. 1999, 2002; Muñoz Caro et al. 2001). Calculations indicate that hydrogenation proceeds at a fast enough rate in the diffuse ISM to balance the dehydrogenation caused by UV photons. Conversely, in dense molecular clouds, the reduced abundance of atomic H and the presence of icy mantles act to prevent rehydrogenation of the grains, which can still be efficiently dehydrogenated by photons and cosmic rays (Mennella et al. 2001, 2003). These and other lines of evidence (e.g., Shenoy et al. 2003) imply that most hydrocarbon-containing grains are formed in the diffuse ISM and that reformation dominates over the dehydrogenation that subsequently occurs, in agreement with the nondetection of the 3.4 μm feature in dense cloud material. This evolutionary scenario for the aliphatic hydrocarbons is entirely consistent with the lack of a 3.4 μm polarization excess in NGC 1068 and several Galactic lines of sight (Adamson et al. 1999; Ishii et al. 2002; Chiar et al. 2006).

6. SUMMARY

We have performed L-band spectropolarimetry of NGC 1068 and shown that the excess polarization over the 3.4 μm feature is below that which would be expected on the basis of the silicate-core/organic-mantle grain model as applied to the Galactic diffuse ISM, consistent with a growing body of evidence suggesting that the aliphatic hydrocarbons in the general diffuse ISM are not formed by processing of the ice mantles that form on silicate grains in molecular clouds. The coated grain model could still be valid in NGC 1068 if there also exists an extra, nonhydrocarbon aligned grain population, or possibly if the grain size distribution is biased to larger sizes than in the diffuse ISM of our Galaxy (detailed calculations of both the continuum and 3.4 μm feature polarization from micron-sized dust grains may be a useful way of constraining the size and/or composition of the carbonaceous grain population in AGNs). Alternatively, reaction of small carbon grains with atomic hydrogen in the diffuse ISM would be expected to produce a population of small, nonpolarizing hydrocarbon-containing grains, which would naturally explain the lack of polarization of the 3.4 μm feature. Such a model is

also successful in accounting for the nondetection of the 3.4 μm band in molecular clouds, which is otherwise difficult to explain.

We would like to thank R. Antonucci, P. Hirst, M. Kishimoto, T. Roush, M. Smith, and A. Tielens for taking the time to comment, and A. Li for providing the optical constants in tabular form. We are grateful to the anonymous referee for comments that strengthened the paper. We thank the Department of Physical Sciences, University of Hertfordshire for providing IRPOL2 for the UKIRT. The United Kingdom Infrared Telescope is operated by the Joint Astronomy center on behalf of the UK Particle Physics and Astronomy Research Council. R. E. M. was supported by the Gemini Observatory, which is operated by the Association of Universities for Research in Astronomy, Inc., on behalf of the international Gemini partnership of Argentina, Australia, Brazil, Canada, Chile, the United Kingdom, and the United States of America.

REFERENCES

Adamson, A. J., Whittet, D. C. B., Chrysostomou, A., Hough, J. H., Aitken, D. K., Wright, G. S., & Roche, P. F. 1999, ApJ, 512, 224
Aitken, D. K., Briggs, G., Bailey, J. A., Roche, P. F., & Hough, J. H. 1984, Nature, 310, 660
Aitken, D. K., Efstathiou, A., McCall, A., & Hough, J. H. 2002, MNRAS, 329, 647
Alloin, D., Pantin, E., Lagage, P. O., & Granato, G. L. 2000, A&A, 363, 926
Antonucci, R. R. J., & Miller, J. S. 1985, ApJ, 297, 621
Bailey, J., Axon, D. J., Hough, J. H., Ward, M. J., McLean, I., & Heathcote, S. R. 1988, MNRAS, 234, 899
Bock, J. J., et al. 2000, AJ, 120, 2904
Bridger, A., Wright, G. S., & Geballe, T. R. 1994, in Infrared Astronomy with Arrays: The Next Generation, ed. I. S. McLean (Dordrecht: Kluwer), 537
Chiar, J. E., Pendleton, Y. J., Geballe, T. R., & Tielens, A. G. G. M. 1998, ApJ, 507, 281
Chiar, J. E., Tielens, A. G. G. M., Whittet, D. C. B., Schutte, W. A., Boogert, A. C. A., Lutz, D., van Dishoeck, E. F., & Bernstein, M. P. 2000, ApJ, 537, 749
Chiar, J. E., et al. 2006, ApJ, 651, 268
Chlewicki, G., & Greenberg, J. M. 1990, ApJ, 365, 230
Clayton, G. C., & Martin, P. G. 1981, AJ, 86, 1518
Dartois, E., Marco, O., Muñoz-Caro, G. M., Brooks, K., Deboffle, D., & d'Hendecourt, L. 2004, A&A, 423, 549
Demyk, K., Dartois, E., D'Hendecourt, L., Jourdain de Muizon, M., Heras, A. M., & Breitfellner, M. 1998, A&A, 339, 553
Draine, B. T. 1985, ApJS, 57, 587
———. 1988, ApJ, 333, 848
Draine, B. T., & Flatau, P. J. 1994, J. Opt. Soc. Am., 11, 1491
———. 2004, preprint (astro-ph/0409262)
Draine, B. T., & Lee, H. M. 1984, ApJ, 285, 89
Efstathiou, A., McCall, A., & Hough, J. H. 1997, MNRAS, 285, 102
García-Gómez, C., Athanassoula, E., & Barberà, C. 2002, A&A, 389, 68
Geballe, T. R., Baas, F., & Wade, R. 1989, A&A, 208, 255
Gibb, E. L., & Whittet, D. C. B. 2002, ApJ, 566, L113
Greenberg, J. M., & Li, A. 1996, A&A, 309, 258
Greenberg, J. M., Li, A., Mendoza-Gomez, C. X., Schutte, W. A., Gerakines, P. A., & de Groot, M. 1995, ApJ, 455, L177
Hao, L., et al. 2005, ApJ, 625, L75
Hildebrand, R. H., & Dragovan, M. 1995, ApJ, 450, 663
Hough, J. H., Whittet, D. C. B., Sato, S., Yamashita, T., Tamura, M., Nagata, T., Aitken, D. K., & Roche, P. F. 1989, MNRAS, 241, 71
Hough, J. H., et al. 1988, MNRAS, 230, 107
Imanishi, M. 2000, MNRAS, 319, 331
———. 2001, AJ, 121, 1927
Imanishi, M., Terada, H., Sugiyama, K., Motohara, K., Goto, M., & Maihara, T. 1997, PASJ, 49, 69
Ishii, M., Nagata, T., Chrysostomou, A., & Hough, J. H. 2002, AJ, 124, 2790
Jaffe, W., et al. 2004, Nature, 429, 47
Kleinmann, D. E., Gillett, F. C., & Wright, E. L. 1976, ApJ, 208, 42
Laor, A., & Draine, B. T. 1993, ApJ, 402, 441
Lazarian, A. 2003, J. Quant. Spectrosc. Radiat. Transfer, 79, 881
Lebofsky, M. J., Kemp, J. C., & Rieke, G. H. 1978, ApJ, 222, 95
Li, A., & Greenberg, J. M. 1997, A&A, 323, 566
———. 2002, ApJ, 577, 789
Lumsden, S. L., Moore, T. J. T., Smith, C., Fujiyoshi, T., Bland-Hawthorn, J., & Ward, M. J. 1999, MNRAS, 303, 209
Maiolino, R., Marconi, A., & Oliva, E. 2001a, A&A, 365, 37
Maiolino, R., Marconi, A., Salvati, M., Risaliti, G., Severgnini, P., Oliva, E., La Franca, F., & Vanzi, L. 2001b, A&A, 365, 28
Marco, O., & Brooks, K. J. 2003, A&A, 398, 101
Mason, R. E., Geballe, T. R., Packham, C., Levenson, N. A., Elitzur, M., Fisher, R. S., & Perlman, E. 2006, ApJ, 640, 612
Mason, R. E., Wright, G., Pendleton, Y., & Adamson, A. 2004, ApJ, 613, 770
Mathis, J. S., Rumpl, W., & Nordsieck, K. H. 1977, ApJ, 217, 425
Matt, G., Fabian, A. C., Guainazzi, M., Iwasawa, K., Bassani, L., & Malaguti, G. 2000, MNRAS, 318, 173
Mennella, V., Baratta, G. A., Esposito, A., Ferini, G., & Pendleton, Y. J. 2003, ApJ, 587, 727
Mennella, V., Brucato, J. R., Colangeli, L., & Palumbo, P. 1999, ApJ, 524, L71
———. 2002, ApJ, 569, 531
Mennella, V., Muñoz Caro, G. M., Ruiterkamp, R., Schutte, W. A., Greenberg, J. M., Brucato, J. R., & Colangeli, L. 2001, A&A, 367, 355
Muñoz Caro, G. M., Ruiterkamp, R., Schutte, W. A., Greenberg, J. M., & Mennella, V. 2001, A&A, 367, 347
Nagata, T., Kobayashi, N., & Sato, S. 1994, ApJ, 423, L113
Packham, C., Young, S., Hough, J. H., Axon, D. J., & Bailey, J. A. 1997, MNRAS, 288, 375
Pendleton, Y. J., & Allamandola, L. J. 2002, ApJS, 138, 75
Pendleton, Y. J., Sandford, S. A., Allamandola, L. J., Tielens, A. G. G. M., & Sellgren, K. 1994, ApJ, 437, 683
Pendleton, Y. J., Tielens, A. G. G. M., Tokunaga, A. T., & Bernstein, M. P. 1999, ApJ, 513, 294
Pendleton, Y. J., Tielens, A. G. G. M., & Werner, M. W. 1990, ApJ, 349, 107
Pogge, R. W., & Martini, P. 2002, ApJ, 569, 624
Rawlings, M. G., Adamson, A. J., & Whittet, D. C. B. 2003, MNRAS, 341, 1121
Rhee, J. H., & Larkin, J. E. 2006, ApJ, 640, 625
Risaliti, G., et al. 2003, ApJ, 595, L17
Roche, P. F., Whitmore, B., Aitken, D. K., & Phillips, M. M. 1984, MNRAS, 207, 35
Sandford, S. A., Allamandola, L. J., Tielens, A. G. G. M., Sellgren, K., Tapia, M., & Pendleton, Y. 1991, ApJ, 371, 607
Sandford, S. A., Pendleton, Y. J., & Allamandola, L. J. 1995, ApJ, 440, 697
Schnaiter, M., Henning, T., Mutschke, H., Kohn, B., Ehbrecht, M., & Huisken, F. 1999, ApJ, 519, 687
Shenoy, S. S., Whittet, D. C. B., Chiar, J. E., Adamson, A. J., Roberge, W. G., & Hassel, G. E. 2003, ApJ, 591, 962
Siebenmorgen, R., Haas, M., Krügel, E., & Schulz, B. 2005, A&A, 436, L5
Simpson, J. P., Colgan, S. W. J., Erickson, E. F., Hines, D. C., Schultz, A. S. B., & Trammell, S. R. 2002, ApJ, 574, 95
Smith, C. H., Wright, C. M., Aitken, D. K., Roche, P. F., & Hough, J. H. 2000, MNRAS, 312, 327
Tinbergen, J. 1996, Astronomical Polarimetry (Cambridge, New York: Cambridge Univ. Press)
Tomono, D., Doi, Y., Usuda, T., & Nishimura, T. 2001, ApJ, 557, 637
van Bemmel, I. M., & Dullemond, C. P. 2003, A&A, 404, 1
Watanabe, M., Nagata, T., Sato, S., Nakaya, H., & Hough, J. H. 2003, ApJ, 591, 714
Weingartner, J. C., & Draine, B. T. 2001, ApJ, 548, 296
Weingartner, J. C., & Murray, N. 2002, ApJ, 580, 88
Wright, G. S., Bridger, A., Geballe, T. R., & Pendleton, Y. 1996, in New Extragalactic Perspectives in the New South Africa, ed. D. L. Block & J. M. Greenberg (Dordrecht: Kluwer), 143
Young, S., Hough, J. H., Axon, D. J., Bailey, J. A., & Ward, M. J. 1995, MNRAS, 272, 513